Reprinted from THE PHYSICAL REVIEW, Vol. 127, No. 4, 1224–1229, August 15, 1962
Printed in U. S. A.

Elastic Scattering of Heavy Ions by Pb^{206}, Pb^{207}, and Pb^{208}†

D. D. KERLEE
Seattle Pacific College Institute for Research, Seattle, Washington
AND
H. L. REYNOLDS AND E. GOLDBERG
Lawrence Radiation Laboratory, University of California, Livermore, California
(Received December 29, 1961; revised manuscript received May 7, 1962)

The angular distributions of C^{12}, N^{14}, O^{16}, and Ne^{20} elastically scattered by Pb^{206}, Pb^{207}, and Pb^{208} have been measured at laboratory energies of approximately 10.4 MeV/nucleon. The elastically scattered ions were recorded in photographic emulsions at laboratory angles from 17° to 175°. In general, measurements were extended only to angles where the ratio of the cross section to the Coulomb cross section, σ/σ_c, was greater than 0.2. In one case, the measurement was extended to a region where $\sigma/\sigma_c \leq 1.2\times10^{-5}$. The cross sections all exhibited a behavior similar to that previously reported for the same ions on Au^{197} and Bi^{209}. Excellent agreement with the semiclassical strong absorption model was obtained. Nuclear interaction distances calculated by fitting the strong absorption calculations are consistent with $r_0=1.45$ F, where $R=r_0(A_1^{\frac{1}{3}}+A_2^{\frac{1}{3}})$.

INTRODUCTION

ELASTIC scattering experiments conducted by Rutherford and subsequent workers[1] formed one of the important bases upon which the nuclear atom was conceived and established. Later, alpha-particle elastic-scattering experiments[2–4] and more recent experiments involving the elastic scattering of heavy ions[5–10] have yielded quantitative information on the respective interaction radii, cutoff values of angular momentum, and values of r_0. Less quantitative information concerning nuclear surface properties has also been obtained. Analysis of the data by means of the semiclassical strong-absorption model, or "sharp cutoff" model, by Blair[3,11,12] has been quite successful in

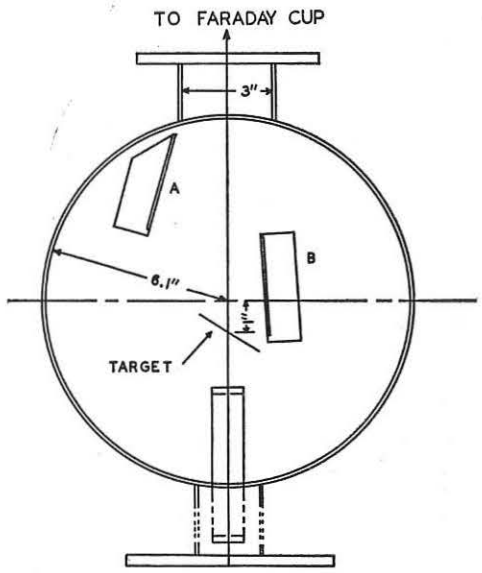

FIG. 1. Positions of emulsions in scattering chamber. Elastic scattering was detected primarily on plate *A*.

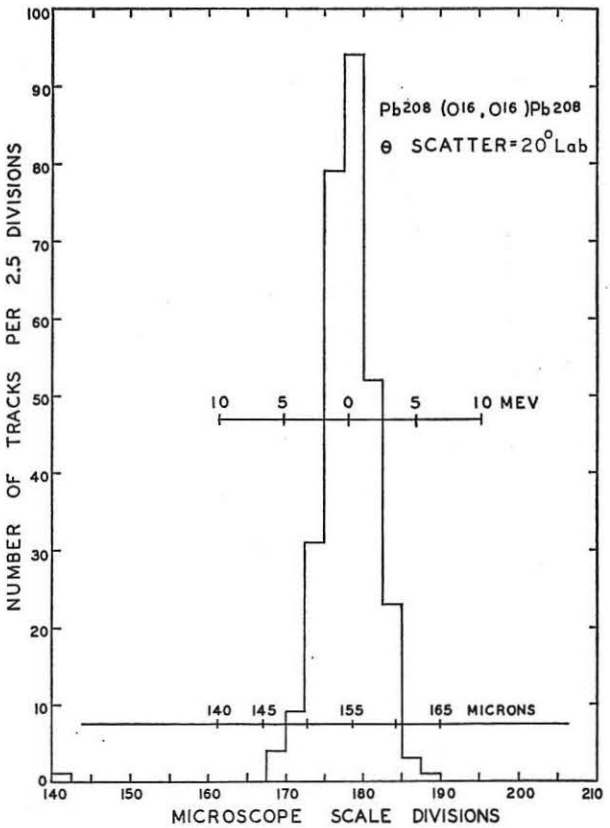

FIG. 2. A typical range spectrum in emulsion for O^{16} ions elastically scattered from Pb^{208} at a scattering angle of 20° in the laboratory. The micron scale has been corrected for track dip angle in the emulsion. The emulsion density is 3.976 g/cc.

† This work has been supported by the U. S. Atomic Energy Commission and by the National Science Foundation.

[1] E. Rutherford and J. Chadwick, Phil. Mag. **50**, 889 (1925).
[2] G. W. Farwell and H. E. Wegner, Phys. Rev. **95**, 1212 (1954).
[3] D. D. Kerlee, J. S. Blair, and G. W. Farwell, Phys. Rev. **107**, 1343 (1957).
[4] Other early alpha particle work is given in reference 3.
[5] H. L. Reynolds and A. Zucker, Phys. Rev. **102**, 1378 (1956).
[6] E. Goldberg and H. L. Reynolds, Phys. Rev. **112**, 1981 (1958).
[7] H. L. Reynolds, E. Goldberg, and D. D. Kerlee, Phys. Rev. **119**, 2009 (1960).
[8] J. A. McIntyre, S. D. Baker, and T. L. Watts, Phys. Rev. **116**, 1212 (1960).
[9] M. L. Halbert and A. Zucker, Phys. Rev. **115**, 1635 (1960).
[10] A. Zucker, Bull. Am. Phys. Soc. **6**, 285 (1961).
[11] J. S. Blair, Phys. Rev. **95**, 1218 (1954).
[12] J. S. Blair, Phys. Rev. **108**, 827 (1957).

TABLE I. Measured ranges and energies for the incident particles.

Reaction	Range[a] (μ)	Energy at emulsion surface (MeV)	Reaction energy (MeV)	E/M (HILAC) (MeV)
$C^{12}+Pb^{206}$	198.6	122.8	124.2	10.38
$N^{14}+Pb^{206}$	175.8	145.0	146.8	10.52
$O^{16}+Pb^{206}$	156.3	164.7	167.1	10.48
$Ne^{20}+Pb^{206}$	130.6	203.6	207.2	10.41
$C^{12}+Pb^{207}$	197.5	122.4	123.7	10.33
$O^{16}+Pb^{207}$	155.1	163.9	166.1	10.41
$Ne^{20}+Pb^{207}$	131.7	204.7	208.1	10.44
$C^{12}+Pb^{208}$	195.1	121.6	122.8	10.26
$N^{14}+Pb^{208}$	176.9	145.7	147.2	10.53
$O^{16}+Pb^{208}$	154.8	163.7	166.0	10.41
$Ne^{20}+Pb^{208}$	129.9	202.8	206.2	10.34

[a] The emulsion density was 3.976 g/cc.

TABLE II. Target thicknesses and isotopic concentrations.

Target	Thickness (mg/cm²)	Isotopic concentration (%)
Pb^{206}	0.97	64.9
Pb^{207}	0.82	71.5
Pb^{208}	0.90	88.9

regions where the "classical" parameter $\eta=zz'e^2/\hbar v$ is large compared to unity.

In the present work, the elastic scattering of C^{12}, N^{14}, O^{16}, and Ne^{20} ions from the lead isotopes, Pb^{206}, Pb^{207}, and Pb^{208}, has been studied using nuclear emulsions. Values of η range from approximately 25 to 40. Angular distributions were obtained for angular intervals from 17° (lab) to an angle such that $\sigma/\sigma_c(\theta)\approx 0.2$. In the case of O^{16} on Pb^{208}, an interval of from 17° to 175° was studied. Upper limits to the value of σ/σ_c were obtained at large angles. At 172° c.m., $\sigma/\sigma_c<1.2\times10^{-5}$.

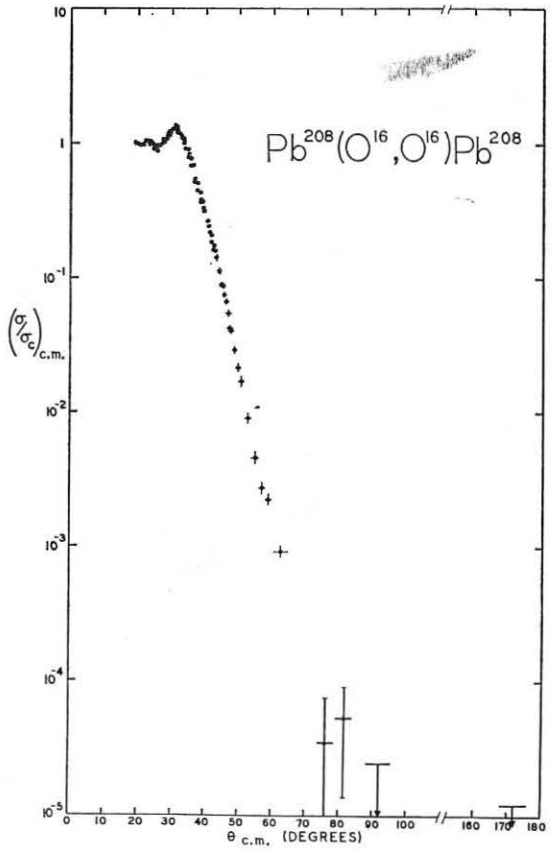

FIG. 3. Ratio of the differential elastic scattering cross section to the Coulomb cross section vs the center-of-mass scattering angle for O^{16} scattered by Pb^{208}. The laboratory energy before scatter is 166.0 MeV. Upper limits to the ratio are indicated at 92° and 172° c.m.

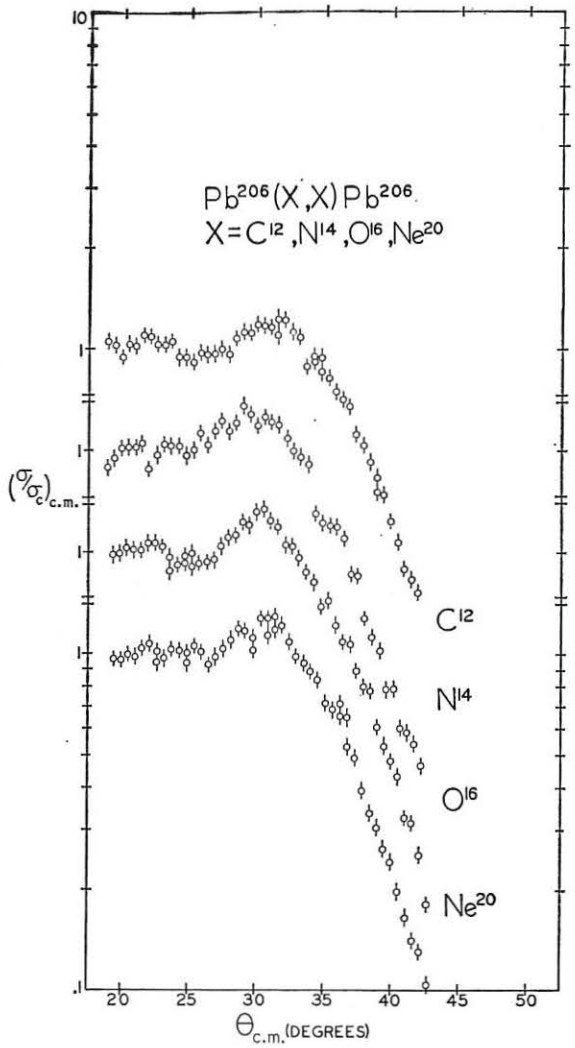

FIG. 4. Ratio of the differential cross section for elastic scattering to the Coulomb cross section vs the center-of-mass angle for C^{12}, N^{14}, O^{16}, and Ne^{20} scattered by Pb^{206}. Relative positions are arbitrary. The curves have been normalized to unity at small angles. Three hundred tracks were counted for each point.

EXPERIMENTAL PROCEDURE

The experimental arrangement has been described in previous papers.[6,7] These papers will be referred to for description of the experimental procedure in the presentation of this further work.

The targets were exposed to heavy-ion projectiles of approximately 10.4 MeV nucleon from the Berkeley heavy-ion linear accelerator (HILAC). The beams from the HILAC were deflected by a bending magnet before they approached the target box (Fig. 1). The distance from the bending magnet to the first collimator slit was approximately $3\frac{1}{2}$ m. The beams passed through two $\frac{1}{8}$-in. diam collimator slits, placed 7 in. apart, before striking the thin targets of isotopic lead. The scattered particles were detected by nuclear emulsions in positions A and B. Position A was loaded with Ilford E-1 emulsions, primarily for detection of elastically scattered particles. Ilford K-2 emulsions in positions B, C, and D (C and D not shown) were used in heavy-ion-induced fission experiments[13] performed simultaneously with the elastic experiments. The K-2 emulsions recorded elastically scattered ions sufficiently well at end of range to obtain elastic angular distributions at position B as well as at A, thus providing elastic angular distribution measurements on either side of the beam axis. The characteristic rapid decrease of the elastic differential scattering cross section with increasing angle allowed a determination of symmetry with the beam axis, thus eliminating all but minor beam-alignment uncertainties.

Factors involving angular resolution have not

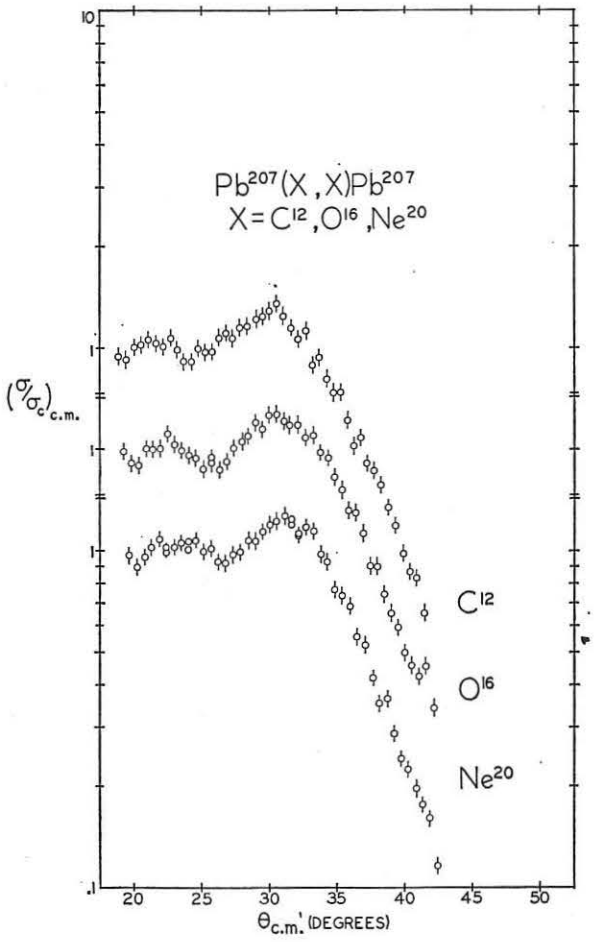

FIG. 5. Ratio of the differential cross section for elastic scattering to the Coulomb cross section vs the center-of-mass angle for C^{12}, O^{16}, and Ne^{20} scattered by Pb^{207}. Relative positions are arbitrary. The curves have been normalized to unity at small angles. Three hundred tracks were counted for each point.

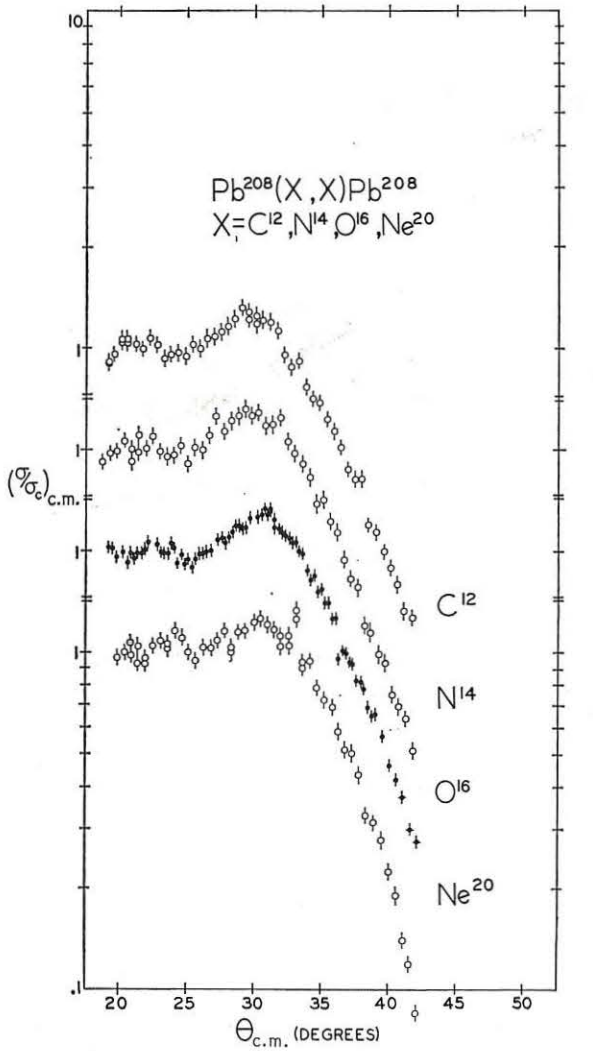

FIG. 6. Ratio of the differential cross section for elastic scattering to the Coulomb cross section vs the center-of-mass angle for C^{12}, N^{14}, O^{16}, and Ne^{20} scattered by Pb^{208}. Relative positions are arbitrary. The curves have been normalized to unity at small angles. One thousand tracks were counted for each point of the O^{16}, Pb^{208} reaction. Three hundred tracks were counted for each point of the other curves.

[13] E. Goldberg, H. L. Reynolds, and D. D. Kerlee, *Proceedings of the Second Conference on Reactions Between Complex Nuclei* (John Wiley & Sons, Inc., New York, 1960), paper D-6, p. 230.

changed appreciably from the earlier report.[7] Contributions to the spread in scattering angle due to initial beam divergence, collimator slit widths, multiple scattering in the target, swath length scanned in the emulsion, and loss of angular resolution due to beam energy, result in a spread in scattering angle of less than $\pm 0.8°$ at half-maximum.

Errors in target box alignment were corrected to within 0.1° by comparison of elastic scattering in plates *A* and *B*. The error in scattering angle due to target box alignment, measurement of the internal geometry of the box, and data processing was $\pm 0.2°$. The above discussion of errors in angle and angular resolution pertains to a range of scattering of from 20° to 40° and applies to particles detected on *A* plate.

The energy of the heavy ions was determined by measuring range spectra and applying the range-energy measurements of Heckman *et al.*[14] The ranges and laboratory energies for scattering from Pb^{206}, Pb^{207}, and Pb^{208} are given in Table I. The incident energy of the projectiles in the laboratory system was approximately 10.4 MeV/nucleon. A magnetic electron suppressor similar to that described earlier[6] was used in these experiments. No rubbing of the emulsion[7] was necessary.

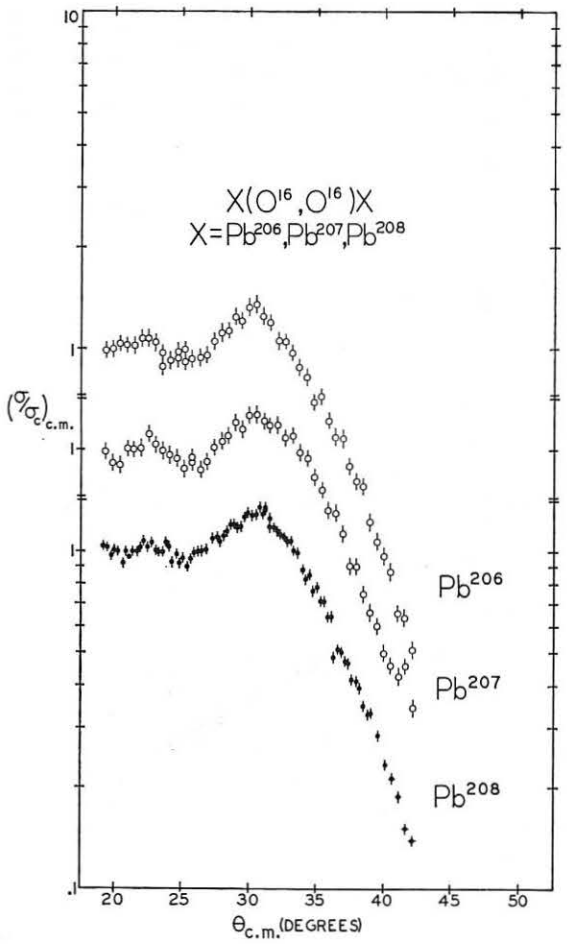

FIG. 7. Ratio of the differential cross section for elastic scattering to the Coulomb cross section vs the center-of-mass angle for O^{16} scattered by Pb^{206}, Pb^{207}, and Pb^{208}. Relative positions are arbitrary. The curves have been normalized to unity at small angles.

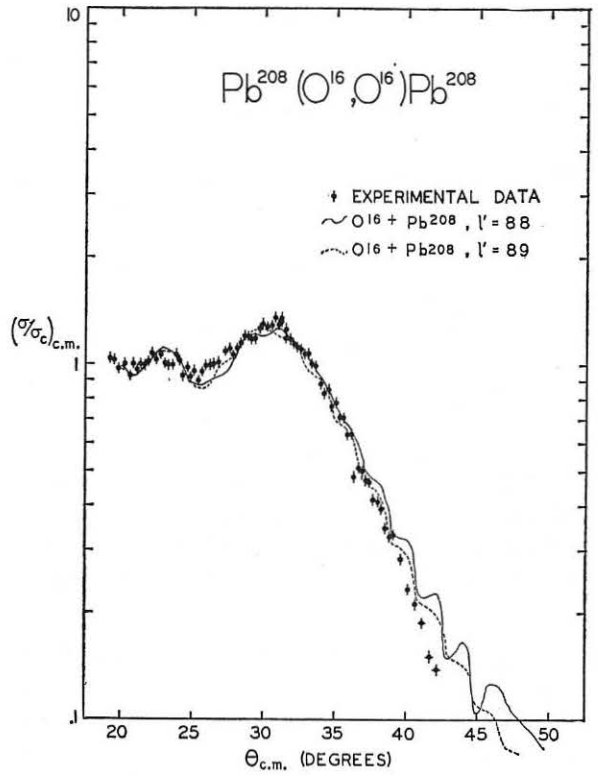

FIG. 8. Ratio of the differential cross section for elastic scattering to the Coulomb cross section vs the center-of-mass angle for O^{16} scattered by Pb^{208}. Sharp-cutoff calculations are shown for $l'=88$, and $l'=89$.

A typical range spectrum of O^{16} on Pb^{208} at a laboratory angle of 20° is shown in Fig. 2. The width is consistent with a range straggling of 1.0% and a standard deviation of the incident-beam energy spread[7] of 1.0%.

The isotopic targets were self-supporting foils of Pb^{206}, Pb^{207}, and Pb^{208}. Isotopic concentrations and target thicknesses are given in Table II. The energy loss of the O^{16} ions in the Pb^{208} target was approximately 1.1 MeV.

RESULTS

In Fig. 3 the experimental angular distribution obtained for O^{16} projectiles incident on Pb^{208} is plotted as the ratio of the differential cross section to the Coulomb cross section, σ/σ_c, vs the center-of-mass angle. It has been assumed that the ratio approaches unity as the scattering angle decreases. At small angles, each point represents 1000 tracks with a resulting

[14] H. H. Heckman, B. L. Perkins, W. G. Simon, F. M. Smith, and W. H. Barkas, Phys. Rev. **117**, 544 (1960).

standard deviation of approximately 3%. Beyond 40° c.m., fewer tracks were measured for each point.

The acceptance angle was broadened for these points to obtain improved sensitivity. The larger standard deviations and angles of acceptance are indicated. No tracks identifiable as elastic, by range and density measurements, were found beyond 82°. Areas scanned are indicated at 92° and 172°. Upper limits to the ratio, σ/σ_c, are indicated on the basis of the areas scanned.

The scattered particle range spectrum has a normal shape up to values of $\sigma/\sigma_c \geqslant 0.2$. Beyond this a broadening of the elastic peak occurs. Consequently, points where $\sigma/\sigma_c < 0.2$ have been determined by accepting only those tracks with the correct range and density for normal elastic scattering. However, it is possible that these points may still contain some nonelastic events. The value of σ/σ_c has an upper limit of 1.2×10^{-5} at 172° c.m.

Composite graphs of the individual experiments are shown in Figs. 4 to 7. With the exception of O^{16} on Pb^{208}, each point represents 300 tracks with a resulting standard deviation of approximately 6%. Figure 4 shows the experimental angular distributions obtained for C^{12}, N^{14}, O^{16}, and Ne^{20} on Pb^{206} plotted as σ/σ_c vs the center-of-mass angle. Figure 5 shows C^{12}, O^{16}, and Ne^{20} on Pb^{207}. Figure 6 shows the four projectiles C^{12}, N^{14}, O^{16}, and Ne^{20} on Pb^{208}. The O^{16}, Pb^{208} experiment is with improved statistics on each point as described above. Figure 7 is a composite of O^{16} on the three lead isotopes.

DISCUSSION

Cutoff values of angular momentum, and values of the nuclear interaction distance have been determined from the Blair model. A representative fit to the experimental data is shown for O^{16} on Pb^{208} in Fig. 8.

TABLE III. Cutoff l' values, nuclear interaction distances, and reaction cross sections.[a]

Reaction	Cutoff l'	Interaction distance R[b] (Fermis)	r_0 (Fermis)	σ_r (barns)
$C^{12}+Pb^{206}$	64.0±1.1	11.8±0.2	1.44±0.02	2.1
$N^{14}+Pb^{206}$	78.0±1.1	12.1±0.2	1.46±0.02	2.3
$O^{16}+Pb^{206}$	89.0±1.7	12.2±0.2	1.45±0.03	2.3
$Ne^{20}+Pb^{206}$	111.5±2.2	12.6±0.2	1.46±0.02	2.4
$C^{12}+Pb^{207}$	65.5±1.1	12.0±0.3	1.46±0.04	2.2
$O^{16}+Pb^{207}$	87.5±1.7	12.2±0.2	1.44±0.02	2.3
$Ne^{20}+Pb^{207}$	112.0±2.2	12.5±0.2	1.45±0.03	2.4
$C^{12}+Pb^{208}$	66.0±1.1	12.1±0.2	1.47±0.02	2.2
$N^{14}+Pb^{208}$	78.0±1.1	12.1±0.2	1.45±0.02	2.3
$O^{16}+Pb^{208}$	88.5±1.7	12.3±0.2	1.45±0.02	2.3
$Ne^{20}+Pb^{208}$	111.5±2.2	12.6±0.2	1.45±0.02	2.4

[a] All errors are probable errors. Uncertainty in the scattering angle due to chamber geometry is included in the cutoff l'-value error.
[b] The value of $E_{c.m.}$ used in the calculation of the interaction distance was the nonrelativistic energy corresponding to the measured (slightly relativistic) reaction energy ($E_{c.m.R}$), where $E_{c.m.}=0.984E_{c.m.R}$. Also the reduced mass was determined from the rest mass of the particles.[7]

The method of analysis is described in previous papers.[6,7] After finding the best-fit l' values, nuclear interaction distances R were obtained from the equation,

$$E_{c.m.}=\frac{Z_1Z_2e^2}{R}+\frac{\hbar^2l'(l'+1)}{2\mu R^2},$$

where μ is the reduced mass. The results are shown in Table III. Values of r_0 were obtained from the relation $R=r_0(A_1^{\frac{1}{3}}+A_2^{\frac{1}{3}})$. The results are consistent with an r_0 of 1.45 F for all of the reactions. Interaction cross sections, computed from the relation

$$\sigma_r=\pi\lambda\!\!\!^{-2}\sum_0^{l'}(2l+1),$$

are also given in Table III.

The error in the radius was determined by the relation[7]

$$|dR|^2=|adE_{c.m.}|^2+|bdl'|^2.$$

The constants a and b for the lead isotopes are shown in Table IV.

Comparisons of the elastic scattering data for O^{16} on Pb^{206}, Pb^{207}, and Pb^{208} indicate no essential difference in the behavior of the rise. This is in contrast to the trend observed with alpha-particle scattering[3] on these isotopes. It was observed with alpha particles that the rise increased as the neutron number N increased from 124 to shell closure at 126. The heavy-ion measurements with larger values of the classical parameter η do not show this trend. Further, a study of the four projectiles on Pb^{208} shows that few distinctive features are revealed by the scan across projectiles. The earlier alpha-particle work indicated a decrease in the rise in the rare-earth region. McIntyre[15] has shown that differences are de-

TABLE IV. Values of constants in error determination for interaction distance.

Reaction	a (Fermis/MeV)	b (Fermis)
$C^{12}+Pb^{206}$	−0.091	0.118
$N^{14}+Pb^{206}$	−0.080	0.103
$O^{16}+Pb^{206}$	−0.073	0.090
$Ne^{20}+Pb^{206}$	−0.060	0.073
$C^{12}+Pb^{207}$	−0.093	0.119
$O^{16}+Pb^{207}$	−0.075	0.091
$Ne^{20}+Pb^{207}$	−0.060	0.074
$C^{12}+Pb^{208}$	−0.093	0.119
$N^{14}+Pb^{208}$	−0.080	0.103
$O^{16}+Pb^{208}$	−0.077	0.091
$Ne^{20}+Pb^{208}$	−0.060	0.073

[15] See reference 13, J. A. McIntyre, S. D. Baker, and K. H. Wang, paper C-8, p. 180.

tectable in the rise and in the oscillations precursory to the rise by comparing the reactions $Pb^{208}(O^{16},O^{16})Pb^{208}$, and $Tb^{159}(F^{19},F^{19})Tb^{159}$. In the present work there is an indication of similar trends in the scan across projectiles (Fig. 6). However, experimental angular resolution and statistics do not allow quantitative evaluation of this effect. Further work in the rare-earth region would be of interest.

ACKNOWLEDGMENTS

We wish to thank the operating crew of the HILAC for their cooperation during exposures. We also would like to thank Dan O'Connell for his help in preparing the targets and Dr. George Farwell and Dr. Arthur Fairhall for the target materials. We are grateful for the assistance of our scanners, Charles Chiu, David Corey, Paul Hsu, and David Yu.